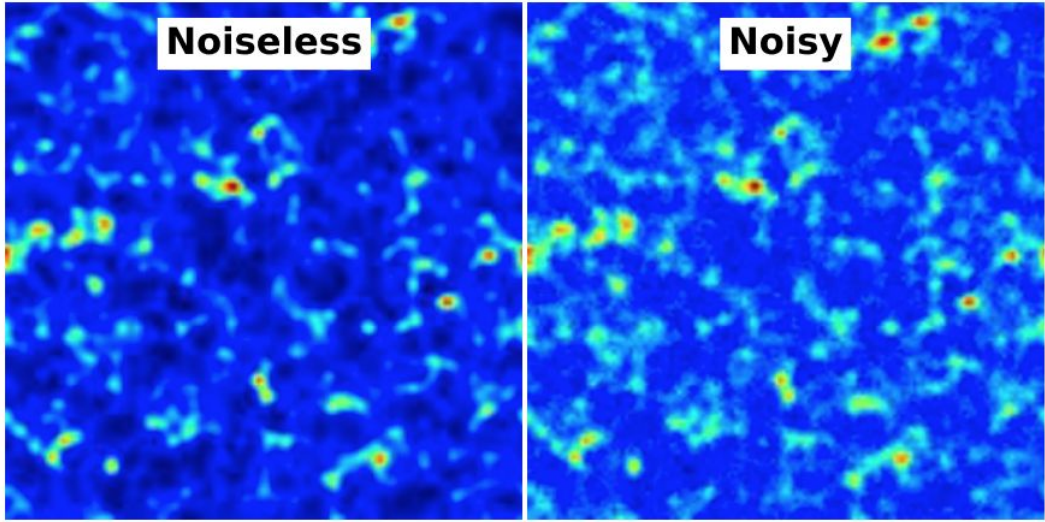


Title:	The Crab Pulsar at Centimeter Wavelengths II: Single Pulses
arXiv:	arXiv:1608.08881
Figure:	<p>The figure consists of two vertically stacked panels sharing a common x-axis labeled 'Time (Microseconds)' ranging from 0 to 6. The top panel is a line plot showing 'Intensity (Jy)' on the y-axis, ranging from 0 to 200. It displays a single, complex pulse with a primary peak of about 200 Jy occurring at approximately 2.2 microseconds. The bottom panel is a dynamic spectrum showing 'Intensity (kJy)' on a color scale from 0 to 2 on the right, plotted against 'Time (Microseconds)' on the x-axis and 'Frequency (GHz)' on the y-axis, ranging from 42 to 44. The dynamic spectrum shows a dispersive tail of the pulse, with the highest intensity (red/yellow) concentrated between 2 and 4 microseconds and 42.5 and 44 GHz. A color bar on the right side of the dynamic spectrum indicates intensity levels from 0 to 2 kJy.</p>
Caption:	<p>The total intensity of a Main Pulse recorded at 43.25 GHz and de-dispersed using DM of 56.794 pc-cm⁻³ (taken from Jodrell Bank monitoring for our observing date) is shown with a time resolution of 44.8 ns. The frequency resolution of the dynamic spectrum is 78 MHz. The Intensity contour levels in the dynamic spectrum are 0.2, 0.5, 1, and 2 kJy. The off-pulse noise level for the total intensity is 15.2 Jy, and for the dynamic spectrum, 110 Jy</p>

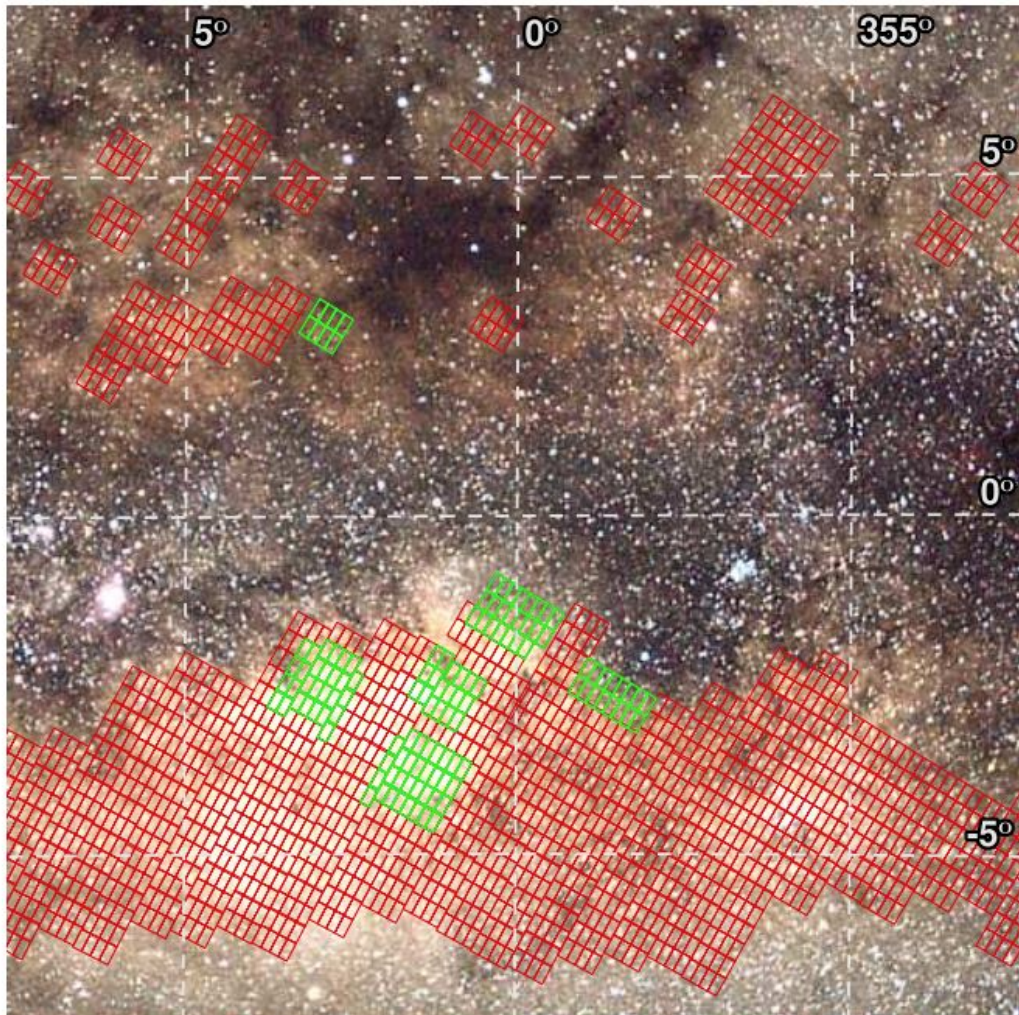
Title:	Towards optimal extraction of cosmological information from nonlinear data
arXiv:	arXiv:1706.06645
Figure:	
Caption:	The truth simulations without (left) and with (right) noise.

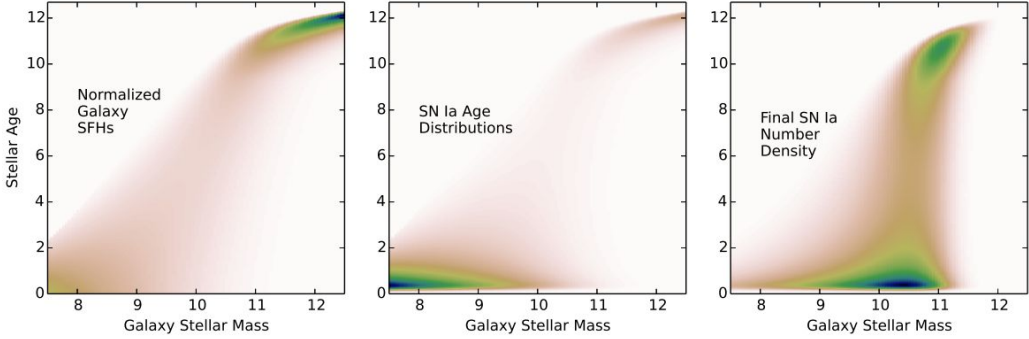
Title:	Merging Galaxies with Tidal Tails in COSMOS to $z=1$
arXiv:	arXiv:1608.04298
Figure:	<p>The figure consists of four panels showing the color-color diagram $U-V$ versus $V-J$ for merging galaxies with long tidal tails. The panels are arranged in a 2x2 grid, corresponding to redshift bins: $0.2 \leq z < 0.4$ (top-left), $0.4 \leq z < 0.6$ (top-right), $0.6 \leq z < 0.8$ (bottom-left), and $0.8 \leq z < 1$ (bottom-right). Each panel displays a large cloud of gray points representing the parent sample of 35,076 galaxies. Overlaid on these are black circles representing galaxies with tidal dwarf galaxy (TDG) candidates and green circles representing galaxies with long tails. Solid lines in each panel indicate the adopted division between quiescent galaxies (above the line) and star-forming galaxies (below the line). A legend in the top-right panel identifies the symbols: black circle for 'gal. with TDG' and green circle for 'gal. with long tail'.</p>
Caption:	<p>The $U - V$ Vs. $V - J$ diagram of 461 merging galaxies with long tidal tails (solid circles) in comparison with the parent sample of 35 076 galaxies (gray points). The black (green) circles represent mergers containing (or not) tidal dwarf galaxy candidates. The solid lines show the adopted division between the star-forming and quiescent galaxies in each redshift bin.</p>

Title:	Interacting galaxies: co-rotating and counter-rotating systems with tidal tails
arXiv:	arXiv:1312.0560
Figure:	<p>The figure consists of six histograms arranged in a 3x2 grid. The left column is labeled 'Galaxies' and the right column is labeled 'AGN'. The top row shows the distribution of redshift (z), the middle row shows the distribution of absolute r-band magnitude ($\log(M_r)$), and the bottom row shows the distribution of stellar mass (M_r). Each plot compares co-rotating pairs (solid blue lines) and counter-rotating pairs (dotted red lines). The y-axis for all plots is the fraction f.</p> <ul style="list-style-type: none"> Top-left (Galaxies, z): The x-axis ranges from 0 to 0.1. The y-axis ranges from 0 to 0.3. Co-rotating pairs peak at $z \approx 0.06$, while counter-rotating pairs peak at $z \approx 0.04$. Top-right (AGN, z): The x-axis ranges from 0 to 0.1. The y-axis ranges from 0 to 0.3. Both samples peak at $z \approx 0.08$. Middle-left (Galaxies, $\log(M_r)$): The x-axis ranges from 9 to 11. The y-axis ranges from 0 to 0.2. Co-rotating pairs peak at $\log(M_r) \approx 10.2$, while counter-rotating pairs peak at $\log(M_r) \approx 10.1$. Middle-right (AGN, $\log(M_r)$): The x-axis ranges from 9.5 to 11.5. The y-axis ranges from 0 to 0.4. Both samples peak at $\log(M_r) \approx 10.8$. Bottom-left (Galaxies, M_r): The x-axis ranges from -18 to -23. The y-axis ranges from 0 to 0.25. Co-rotating pairs peak at $M_r \approx -20.2$, while counter-rotating pairs peak at $M_r \approx -20.1$. Bottom-right (AGN, M_r): The x-axis ranges from -19 to -23. The y-axis ranges from 0 to 0.3. Both samples peak at $M_r \approx -20.8$.
Caption:	<p>Distribution of redshift (top), absolute r-band magnitude (middle) and stellar mass content (bottom) for the non-AGN galaxy sample (left) and for the AGN galaxy sample (right) in co and counter-rotating pairs. The solid lines correspond to the co-rotating and the dotted lines correspond to the counter rotating galaxy pairs, respectively.</p>

Title:	OMEGA - OSIRIS Mapping of Emission-line Galaxies in A901/2: III. - Galaxy Properties Across Projected Phase Space in A901/2
arXiv:	arXiv:1706.05199
Figure:	<p>The figure consists of three panels. The left panel is a histogram showing the distribution of the difference between prism and spectroscopic redshifts, $z_{\text{prism}} - z_{2\text{dF,VIMOS}}$. The x-axis ranges from -0.04 to 0.02, and the y-axis (Number) ranges from 0 to 60. The distribution is centered around 0, with a median offset of -0.004. The middle panel is a scatter plot of $z_{2\text{dF,VIMOS}}$ versus z_{prism} for $z_{\text{prism}} \geq 0.12$ (N=143). The x-axis is z_{prism} and the y-axis is $z_{2\text{dF,VIMOS}}$, both ranging from 0.12 to 0.24. A solid black line represents $y = x$, and a dashed red line represents a linear fit to the data, $y = 0.65x + 0.06$. The right panel is a scatter plot of $z_{2\text{dF,VIMOS}}$ versus $z_{\text{prism,corrected}}$, labeled "Post correction". The axes are the same as in the middle panel. The data points are now more tightly clustered around the solid black line $y = x$, indicating improved agreement between the two redshift measurements after correction.</p>
Caption:	<p>This figure compares the spectroscopic and prism redshifts for a subset of 143 galaxies having both kinds of redshifts. The left panel shows the distribution of offsets between the spectroscopic and prism redshifts. The middle panel shows that the offset is redshift dependent. The solid line is $y = x$. The dashed line is a fit to the data. In the right panel, we have used the fit from the middle panel to recalibrate the prism redshifts to better match the spectroscopic redshifts.</p>

Title:	OMEGA - OSIRIS Mapping of Emission-line Galaxies in A901/2: III. - Galaxy Properties Across Projected Phase Space in A901/2
arXiv:	arXiv:1706.05199
Figure:	
Caption:	The top panel shows the spatial distribution of the 856 galaxies in sample S2 coded by the source of the adopted redshifts. The four subclusters are separately labelled, and their spheres of influence (R_{200}) are shown as circles.

Title:	Interstellar extinction curve variations towards the inner Milky Way: a challenge to observational cosmology
arXiv:	arXiv:1510.01321
Figure:	 An optical image of the Galactic bulge showing a dense field of stars. Overlaid on the image are numerous rectangular subfields, most of which are outlined in red. A few subfields are outlined in green. The image includes a dashed white grid representing Galactic coordinates. Labels for Galactic longitude (l) are placed at the top: 5°, 0°, and 355°. Labels for Galactic latitude (b) are placed on the right side: 5°, 0°, and -5°.
Caption:	Subset of OGLE-III subfields shown in red overlaid on an optical image of the Galactic bulge with Galactic coordinate system shown as well. The subfields used in this work, for which we also use the matching V V V photometry, are shown in green.

Title:	Ages of Type Ia supernovae over cosmic time
arXiv:	arXiv:1409.2951
Figure:	 <p>The figure consists of three heatmaps arranged horizontally. Each plot has 'Stellar Age' on the vertical axis (ranging from 0 to 12) and 'Galaxy Stellar Mass' on the horizontal axis (ranging from 8 to 12). - The left plot, titled 'Normalized Galaxy SFHs', shows a broad distribution of stellar ages across the stellar mass range, with higher density at lower ages and lower stellar masses. - The middle plot, titled 'SN Ia Age Distributions', shows a similar broad distribution but with a distinct concentration of older stars (ages 8-12) at higher stellar masses. - The right plot, titled 'Final SN Ia Number Density', shows a very sharp concentration of Type Ia supernovae at high stellar masses (around 11-12) and high stellar ages (around 10-12), with a secondary, smaller concentration at lower stellar masses and lower ages.</p>
Caption:	<p>Left: Normalized mean galaxy SFHs as a function of total stellar mass. Middle: SN Ia age distribution versus host galaxy mass (not re-normalized: age distribution per unit mass). Right: Intrinsic distribution of SNe Ia in progenitor age-host mass space in the local Universe ($z = 0$).</p>

Title:	Linking the structural properties of galaxies and their star formation histories with STAGES
arXiv:	arXiv:1510.01115
Figure:	<p>The figure consists of four panels, each representing a different galaxy morphology: E (top-left), S0 (top-right), Sp (bottom-left), and Irr (bottom-right). Each panel contains a scatter plot and two histograms. The scatter plots show the relationship between the specific star formation rate (SSFR) and the color index $\Delta(W_{462} - W_{518})$. The y-axis for all scatter plots is $\log(\text{SSFR yr}^{-1})$, ranging from -12 to -9. The x-axis is $\Delta(W_{462} - W_{518})$, ranging from -1.0 to 0.5. The histograms show the distribution of SSFR (top histogram) and $\Delta(W_{462} - W_{518})$ (bottom histogram). The SSFR histogram y-axis is 'Norm. Counts' from 0.0 to 1.2. The $\Delta(W_{462} - W_{518})$ histogram y-axis is 'Norm. Counts' from 0.0 to 1.2. The histograms are color-coded: black dashed line for relaxed galaxies, blue solid line for disturbed galaxies, and red histogram for visual mergers. The SSFR histogram excludes objects with only SFR upper or lower limits. The $\Delta(W_{462} - W_{518})$ histogram includes all objects.</p>
Caption:	<p>Specific SFR vs. $\Delta(W_{462} - W_{518})$ for cluster galaxies of all morphologies. As in Fig. 2, black squares correspond to relaxed systems, blue circles to disturbed galaxies not classified as mergers and red symbols to visual mergers. Objects with only SFR upper or lower limits are presented as pluses with appropriate colours. In the accompanying histograms, the black dashed line shows the relaxed galaxies, the blue solid line the disturbed ones, and the red histogram the visual mergers. The SSFR histogram excludes objects with only SFR upper or lower limits. The $\Delta(W_{462} - W_{518})$ histogram includes all objects. In all cases, the histograms are normalized to a maximum value of one in order to amplify the differences between the distribution functions.</p>

